# Wavefront Reconstruction With Fresnel Holograms by Arbitrary Phase-step Digital Holography

Wang-Ta Hsieh<sup>1</sup>, Ming-Kuei Kuo<sup>2</sup>, and Chi-Ching Chang<sup>\*3</sup>

School of Defense Science, National Defense University
 Department of Electronic & Electrical Engineering, National Defense University
 Institute of Electro-Optical Engineering, Ming Dao University

#### **ABSTRACT**

The principle of wavefront reconstruction by arbitrary phase-step digital holography using Fresnel holograms is presented. Using the inherent nature of the in-line geometry in digital holography, the arbitrary phase-step of the reference wave can be easily estimated. The object wavefront can be numerically reconstructed without twin-image blurring using only two holograms, allowing the number of holograms to be reduced and the optical setup further simplified. Computer simulations are carried out to verify the proposed approach. Optical experiments are performed to validate the approach. The optical results and spatial resolutions between different numbers of recorded holograms are also presented and discussed.

**Keywords:** digital holography, arbitrary phase-step, wavefront reconstruction, twin-image blurring.

# 利用菲涅耳全像片及任意相位步進數位全像術進行波形重建

謝旺達 郭明貴 張冀青3\*

<sup>1</sup>國防大學理工學院國防科學研究所 <sup>2</sup>國防大學理工學院電機系 <sup>3</sup>明道大學光電工程研究所

# 摘 要

本文提出利用多張菲涅耳全像片及任意相位步進數位全像術波形重建的原理。利用數位全像術同軸光路的基本特性,在光路中參考光所改變之相位步進可以很容易地估計。只要記錄兩張全像片,物體波前可以數值法重建,同時沒有零階與共軛影像的干擾,如此可簡化光路設置,以及全像片張數。為證實所提方法可行性,我们以電腦模擬及光學實驗確認之。最後,展示與討論在記錄不同張數的全像片之間的光學結果與系統的空間解析能力。

**關鍵詞:**數位全像術,任意相位步進,波形重建,共軛像干擾

文稿收件日期 98.08.05; 文稿修正後接受日期 99.03.23;\*通訊作者 Manuscript received August 05, 2009; revised March 23, 2010;\* Corresponding author

#### I. INTRODUCTION

In digital holography (DH) the hologram is digitized and the object wavefront is numerically reconstructed using a computer. This idea was proposed by Goodman and Lawrence [1]. This technique has received increasing attention since a CCD camera was used to directly acquire a Fresnel hologram by Schnars and Juptner [2]. This method, the so-called DH, enables full digital hologram recording and processing without chemical or physical developing, thus increasing the flexibility and speed of the experimental process. Those digital holograms were recorded using off-axis geometry. However, because of the angle between the reference and object waves, off-axis DH does not use the available CCD space-bandwidth product.

In-line geometry was developed to eliminate these limitations. However, as with in-line classical holography, the major restraint of in-line geometry is produced by the dc term and twin-image during numerical reconstruction. This causes blurring. Blurring suppression has become the primary DH research issue. Various experimental setups and numerical algorithms have been proposed to suppress the unwanted noise [3-13]. The simplest solution of these methods is digital in-line holography (DIH) [6-8], which requires a laser, a pinhole and a CCD. The distance of the CCD from the pinhole. typically a few centimeters, was adjusted to capture all interference fringes of the hologram that could be resolved with sufficient pixels. The micrometer-sized (or sub micrometer-sized) object to be visualized was located a distance, typically a few millimeters from the pinhole, such that the Fraunhofer or far-field condition was fulfilled [14]. Using this simple setup, the image on the screen was dominated by its holographic part, and the twin-image did not create problem during numerical reconstruction, since it only caused some quite minor variations of intensity across the real image and reduced to a constant for the far-field approximation [14]. It must be pointed out; however, the method is not applicable to the objects whose dimensions are larger than millimeters due to the limitations imposed by the far-field condition. Note that when the wavelength of incident light  $\lambda = 0.6328 \mu m$ , the far-field of an object of diameter 1 mm starts at

about 40 *m*, which is impossible to fulfill in laboratory environment. Therefore, to remove the limitations imposed by the far-field condition and thus save the optical space, the more complex optical setups than DIH, e.g. the phase-shifting technique [9] or the arbitrary phase-steps methods [10-13], are needed to reconstruct the object wavefront with multiple Fresnel holograms in the Fresnel or near-field region.

To eliminate the undesirable images, Yamaguchi and Zhang [9] proposed four Fresnel holograms with phase shifts of 0,  $\pi/2$ ,  $\pi$  and  $3\pi/2$  of the reference wave by employing a piezoelectric transducer (PZT) mirror. Because the conventional phase-shifting DH requires a special and constant phase shift,  $2\pi/N$ , where the integer  $N \ge 3$ , this requirement is often difficult to precisely meet in reality. Therefore, we present an arbitrary phase-steps DH (APSDH) with multiple holograms (at least two) to suppress the blurring using different approaches, e.g. blind searching algorithm [11], limited area algorithm [12, 13], to estimate the phase-steps of the reference wave.

This paper will present the principle and algorithm for APSDH using multiple holograms, which is the extension of the approach of Hsieh et al. [12, 13]. The proposed approach is re-described using the following statement for convenience. After recording the holograms with/without a phase step, the dc term is first suppressed from these two holograms using the Kreis et al. or Chen et al. or typical methods [3-5]. The phase-step is then a function related to the ratio of reduced intensities of the two holograms and phase differences between the object and reference waves. For further approximation, the phase change due to the object illuminated by the object beam is neglected. The phase differences (i.e. optical path difference) between the object and reference waves can be calculated using simple argument. From the calculated phase differences, the tangent values of them which are very small compared to one (<<1) can be found near optical axis. The contribution of the tangent values can be neglected from the ratio of "reduced" intensities between the two holograms. Then the phase-step can be easily estimated in the space or spatial frequency domain, allowing use of the estimated phase-step with the two reduced

hologram intensities to numerically reconstruct the object wavefront. Simulations are carried out to verify the proposed approach by using the resolution target as the input image (1024 × 1024 pixels in size). Optical experiments are performed to validate the approach with a resolution target as an object. The optical results and spatial resolutions between different numbers of recorded holograms are also presented and discussed.

# II. PRINCIPLE AND ALGORITHM

In DH (as shown in Fig. 1), a second wave with known amplitude and phase, mutually coherent with the first is used as the reference wave. The reference wave,  $\psi_R$ , interferes with the object wave,  $\psi_O$ , produced by the light passing through or reflected by the object.

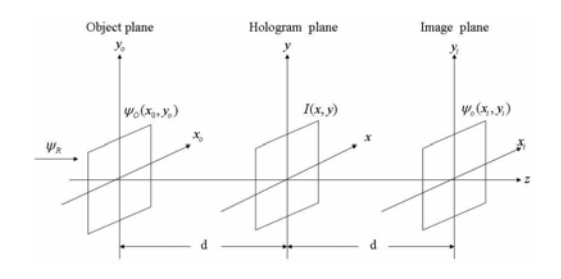


Fig. 1. Geometry for in-line digital holography.

In APSDH, the intensities of the two holograms at the hologram plane can be expressed as

$$I_{HI}(x,y) = |\psi_{o}(x,y) + \psi_{R}(x,y)|^{2}$$

$$= |\psi_{o}|^{2} + |\psi_{R}|^{2} + \psi_{o}\psi_{R}^{*} + \psi_{o}^{*}\psi_{R}$$

$$= a_{o}^{2} + a_{r}^{2} + 2a_{o}a_{r}\cos[(\varphi_{o}(x,y) - \varphi_{r}(x,y))]$$
(1)

$$I_{H2} = a_a^2 + a_r^2 + 2a_a a_r \cos(\varphi_a - \varphi_r - \Delta\varphi)$$
 (2)

where  $a_o$ ,  $a_r$ ,  $\varphi_o$ ,  $\varphi_r$  denote the amplitudes and phases of complex fields  $\psi_O$ ,  $\psi_R$ , respectively. (x, y) denote the coordinates of the hologram plane coordinates and  $\Delta\varphi$  the arbitrary phase-step of the reference wave, respectively. On the right hand side of Eq. (1), the first two terms correspond to the dc term, the third term to the original object wavefront and the fourth to the twin-image.

#### 2.1 Suppression of dc term

The dc term will be suppressed using one of the following methods. It can be removed using the experimental method or the numerical method or the combined method.

#### Method A – four recording holograms

The object wave and reference wave beams are blocked separately [5], such that the intensities of the object wave  $|\psi_o|^2$  and reference wave  $|\psi_R|^2$  can be recorded at the hologram plane. The dc term can then be subtracted from the holograms 1 and 2.

$$I'_{HI} = I_{HI} - |\psi_R|^2 - |\psi_O|^2 \tag{3}$$

## Method B - three recording holograms

The intensity of the reference wave is also recorded by blocking the object wave beam. The dc term can be suppressed using the method proposed by Chen et al. [4] to approximate the intensity of the object wave.

$$I_{HI} = I_{HI} - \left| \psi_R \right|^2 - \frac{\left( I_{HI} - \left| \psi_R \right|^2 \right)^2}{I_{HI} + \left| \psi_R \right|^2} \tag{4}$$

### Method C- two recording holograms

We can calculate the average intensities of the hologram 1 and 2 and subtract this average intensity from both holograms using the Kreis and Juptner method [3].

$$I'_{H1} = I_{H1} - \frac{1}{NM} \sum_{k=1}^{N} \sum_{l=1}^{M} I_{H1}(k, l)$$
 (5)

Utilizing the above methods, the dc term can be completely suppressed and the intensity of the first hologram reduced. It can now be written as

$$I'_{HI} = \psi_o \psi_R^* + \psi_o^* \psi_R$$
  
=  $2a_o a_r \cos(\varphi_o - \varphi_r)$  (6)

Similarly after the dc term is completely suppressed, the reduced intensity of the second hologram can be written as

$$I'_{H2} = \psi_O \psi_R^* \exp(-j\Delta\varphi) + \psi_O^* \psi_R \exp(j\Delta\varphi)$$

$$= 2a_o a_o \cos(\varphi_O - \varphi_O - \Delta\varphi).$$
(7)

## 2.2 Elimination of twin-image blurring

Let Eq. (7) be multiplied by the term of  $\exp(-j\Delta\varphi)$ , it is then subtracted using Eq. (6). We can obtain the following expression as

$$I'_{HI} - \exp(-j\Delta\varphi)I'_{H2}$$

$$= [1 - \exp(-j2\Delta\varphi)]\psi_{\alpha}\psi_{\alpha}^{*}$$
(8)

Since  $\Delta \varphi$  can be considered fixed during the recording stage, so that the term  $[1 - \exp(-j2\Delta\varphi)]$  is a constant. Now it can be found that the right-hand side of Eq. (8) contains only the product of the object wave and the conjugate of the reference wave, thus the twin-image is eliminated and disappeared from above numerical operations. Then the object wavefront in the image plane can be reconstructed using the convolution approach [15] as

$$\psi_O \psi_R^* = \mathfrak{F}^{-1} \{ \mathfrak{F} \{ U \} \mathfrak{F} \{ h(z=d) \} \}$$
 (9)  
, where  $U = I'_{HI} - \exp(-j\Delta \varphi) I'_{H2}$  and  $h(z=d)$  represents the impulse response through distance  $z=d$ , respectively.

#### 2.3 Estimation of arbitrary phase-step $\Delta \varphi$

From Eq. (8), we need to estimate the value  $\Delta \varphi$  to reconstruct the object wavefront. If the phase-step can be accurately estimated, the image can then be numerically reconstructed without blurring. In general,  $\Delta \varphi$  can be estimated from the two recorded holograms using the well known phase-retrieval algorithms [16]. However, those algorithms are always time consuming in executing iteration schemes. Conversely, we will present a totally different approach (compared with those algorithms), that uses the inherent nature of in-line geometry to estimate the phase-step more accurately.

From Eqs. (7) and (6), the ratio of the reduced intensities between  $I'_{H_2}$  and  $I'_{H_1}$  can expressed as

$$\frac{I'_{H2}}{I'_{H1}} = \cos(\Delta \varphi) + \tan(\varphi_o - \varphi_r) \sin(\Delta \varphi) \quad (10)$$

The digital representation of hologram  $I'_{H}(k,l)$  results from 2-D spatial sampling of  $I'_{H}(x,y)$  by CCD and is expressed as [17]

$$I'_{H}(k,l) = I'_{H}(x,y)rect\left(\frac{x}{N\Delta x}, \frac{y}{M\Delta y}\right)$$

$$\times \sum_{k=1}^{N} \sum_{l=1}^{M} \delta(x - k\Delta x, y - l\Delta y)$$
(11)

, where  $\Delta x = Lx / N$  and  $\Delta y = Ly / M$  are the sampling intervals in the hologram plane,  $N \times M$  is the number of light-sensitive pixels on the CCD. The Lx and Ly denote the width of the CCD array in the x- and y- direction, respectively.

If the value of the  $\tan(\varphi_o - \varphi_r)$  term can be neglected for some area of the hologram plane, Eq. (10) can then be further simplified and the phase-step can be easily estimated. For the in-line holography configuration some area exists near the hologram plane optical axis in which their  $\tan(\varphi_o - \varphi_r)$  term can be neglected with simple argument. We show this by calculating the phase differences between the object and reference waves.

For simplicity, we only consider the 1-D case (*x*-direction) as shown in Fig. 2.

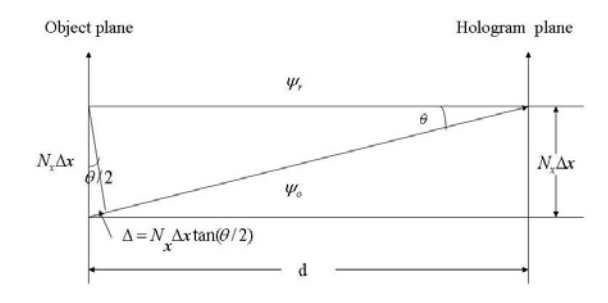


Fig. 2. Geometry of the object wave and reference wave near optical axis.

It is straightforward to express the phase difference near the optic axis as

$$\varphi_{o} - \varphi_{r} = \frac{2\pi}{\lambda} \Delta = \frac{2\pi}{\lambda} N_{x} \Delta x \tan(\theta/2)$$

$$\approx \frac{\pi}{\lambda} \frac{(N_{x} \Delta x)^{2}}{d}$$
(12)

, where d is the distance between object plane and hologram plane,  $N_x$  the pixel number,  $\Delta x$  the pitch size along x-direction and  $\lambda$  wavelength, respectively. According to our experimental setup, we choose these parameters as follows: d = 10 cm,  $\Delta x = 4.67 \mu m$  (from the specification of the Pixera-150SS CCD camera) and  $\lambda = 10 \text{ cm}$ 

 $0.6328\mu m$ . We can substitute these values into Eq. (12) and obtain the values of the phase difference which are proportional to the square of the pixel number  $N_x$ . To satisfy the condition of  $\tan(\varphi_o - \varphi_r) << 1$ , we choose  $\varphi_o - \varphi_r < 5^\circ$  (i.e.  $\tan(\varphi_o - \varphi_r) \cong 0.08749$ ), and the pixel number  $N_x$  can then be estimated to be less than 10, as shown in Fig. 3.

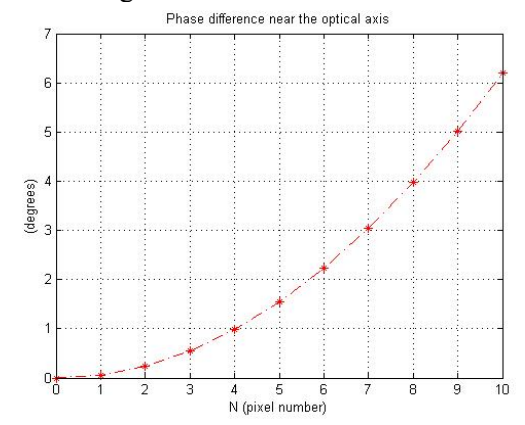


Fig. 3. Phase difference between the object and reference waves near the optical axis.

From the above simple argument, then Eq. (10) can now be rewritten (in discrete form) as

$$\frac{I'_{H2}(k,l)}{I'_{HI}(k,l)} \cong \cos \Delta \varphi$$

for 
$$\begin{cases} N/2 - N_x/2 < k < N/2 + N_x/2 \\ M/2 - M_y/2 < l < M/2 + M_y/2 \end{cases}$$
 (13a)

$$\frac{I'_{H2}}{I'_{HI}} = \cos(\Delta \varphi) + \tan(\varphi_o - \varphi_r) \sin(\Delta \varphi)$$

others 
$$k$$
.  $l$ . (13b)

From Eq. (13a), the value  $\Delta \varphi$  of every pixel near the optical axis can be estimated easily. Alternatively,  $\Delta \varphi$  can be estimated using the Fourier transform ratio of their reduced

intensities with the same approximations,

$$\Im\{I'_{H}(k,l)\} = \sum_{k=0}^{N-1} \sum_{l=0}^{M-1} I'_{H}(k,l) \exp[-j2\pi(uk/N + vl/M)]$$
(14)

where u = 0, ..., N-1 and v = 0, ..., M-1.

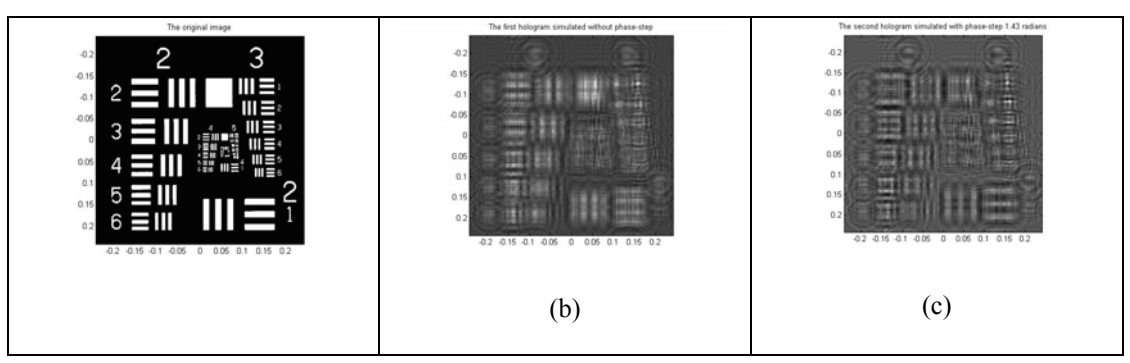
$$\frac{\Im\left\{I_{H_{1}}^{\prime}\right\}}{\Im\left\{I_{H_{1}}^{\prime}\right\}} = \frac{\Im\left\{2a_{o}a_{r}\cos(\varphi_{o} - \varphi_{r} - \Delta\varphi)\right\}}{\Im\left\{2a_{o}a_{r}\cos(\varphi_{o} - \varphi_{r})\right\}} \cong \cos(\Delta\varphi)$$
(15)

for the same limitation as Eq. (13a).

# III. COMPUTER SIMULATIONS AND DISCUSSIONS

In this section, we perform simulations to test the proposed approach. In the simulation procedure the intensity ratio of the object wave to reference wave is assumed to be 1:1. The original image ( $1024 \times 1024$  pixels in size) is shown as in Fig. 4(a). The reference wave is a plane wave. As described in Section 2, the simulated distance between the object plane and hologram plane is d=10.0cm and the illumination wavelength  $\lambda=0.6328\mu m$ . The phase-step  $\Delta \varphi$  is set to be 1.43 radians.

Figures 4(b) and 4(c) show the two holograms simulated with/without the phase-step, respectively. Using one of the three methods as described in Section II, the dc term can be suppressed from the two holograms. The value  $\Delta\varphi$  can then be estimated from Eqs. (13a) or (15) with the pixel array (505:517, 505:517) near the optical axis. The optimal estimated values  $\Delta\varphi$  using these three methods are shown in Table 1.



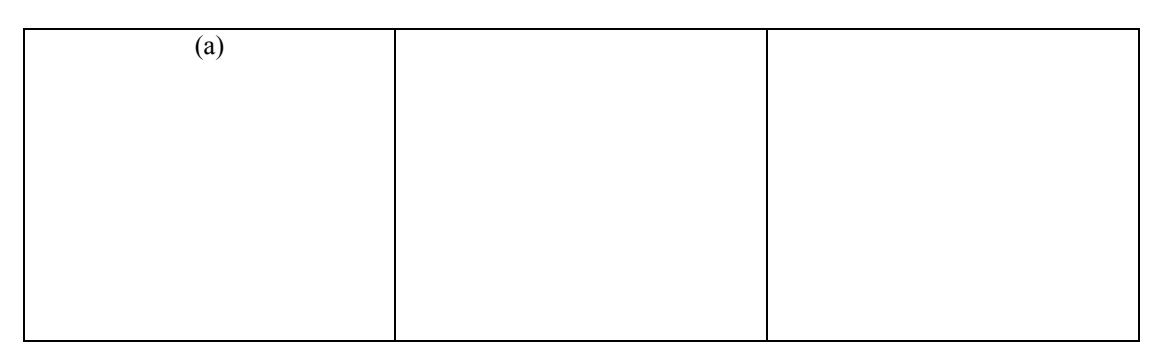


Fig. 4. Simulation results: (a) Original image, (b) First hologram, (c) Second hologram.

	Method A	Method B	Method C	
	(spatial domain)	(frequency domain)	(frequency domain)	
phase-step $\Delta \varphi$	1.4324	1.4113	1.5303	
(radians)				
Error (%)	0.17%	1.3%	7.01%	

Table 1. Estimated phase-step  $\Delta \varphi$  by computer simulations

Figures 5(a), 5(b) and 5(c) show the numerically reconstructed image using Eq. (9) and those three methods, respectively. It can be found that those three methods can all be used to

numerically reconstruct the object wavefront without obvious blurring.

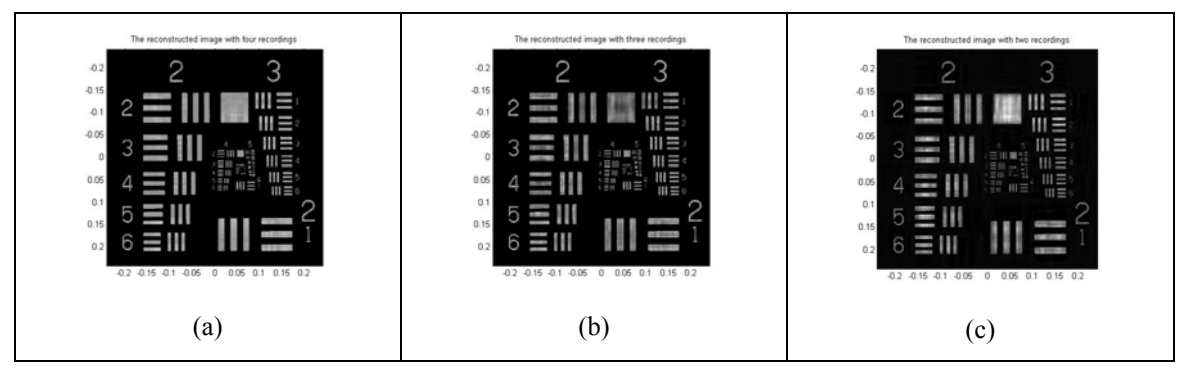


Fig. 5. Reconstructed images by simulations with: (a) Method A, (b) Method B, (c) Method C.

Naturally, the method A is the best scheme to suppress the dc term and twin-image, but it needs the longest time to record the four recordings. Using it, the dc term is completely eliminated from the two holograms, so the optimal value  $\Delta \varphi$  can be estimated with error as little as 0.17%. The image can then be numerically reconstructed accurately without blurring. Unlike method A, the optical setup of method B with three recordings is simpler, but the dc term is not completely eliminated as in

method A. The quality of the reconstructed image is therefore not better than that produced by method A. The optimal value  $\Delta \varphi$  is better estimated in the frequency domain (using Eq. (15)) with error as little as 1.3%, which is greater than that from method A. Although method C with two recordings is the simplest and shortest time among them, as expected, the optimal value  $\Delta \varphi$  has about 7.0% greater error than the others.

# IV. EXPERIMENTAL SETUP AND RESULTS

The Mach-Zehnder setup as shown in Fig. 6 is performed to validate the proposed approach. The arbitrary phase-step of the reference wave in the optical path was obtained by inserting a glass. The two holograms, object wave and reference waves were recorded by a CCD sensor (Pixera-150SS CCD camera,  $1040 \times 1392$  pixels,  $0.484cm \times 0.65cm$ ), respectively. A resolution target (size 1.0  $cm \times 1.0cm$ ) was chosen as an object to evaluate the spatial resolution of the proposed optical system, and placed at a distance of z=12.40cm away from the CCD.

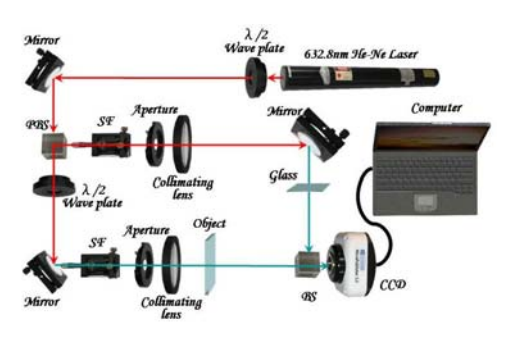


Fig. 6. Schematic of Mach-Zehnder setup.

Figures 7(a) and 7(b) show the two holograms with/without the phase-step captured by CCD at the hologram plane, respectively. Using one of the three methods as described in Section 2, the dc term can be suppressed from the two holograms. The value  $\Delta\varphi$  can then be estimated from Eqs. (13a) or (15) with the pixels array (515:525, 691:701) near the optical axis. The optimal estimated values of  $\Delta\varphi$  using these three methods are shown in Table 2.

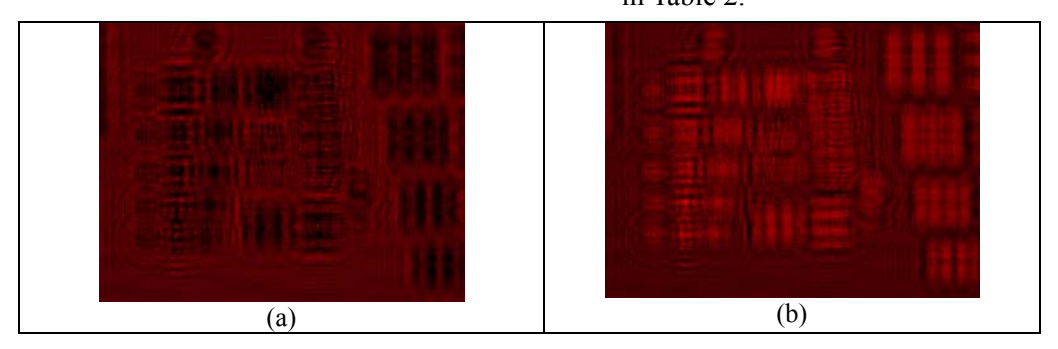


Fig. 7. Optical experimental results: (a) First digital hologram, (b) Second digital hologram.

Table 2. Estimated phase-step  $\Delta \varphi$  and spatial resolution by optical results

	Method A	Method B	Method C
	(frequency domain)	(frequency domain)	(frequency domain)
phase-step $\Delta \phi$	1.5614	1.5444	1.5402
(radians)			
cut off spatial	45.25cycle/mm	45.25cycle/mm	40.32cycle/mm
frequency			
spatial resolution	11.05μm	11.05μm	12.40μm

Figures 8(a), 8(c) and 8(e) show the numerically reconstructed image of resolution target using Eq. (9) and methods A, B and C,

respectively. Unlike the simulation results, which are generated from a man-made, well controlled and super artificial environment, only

the reconstructed images in Fig. 8(a) using method A can be found without obvious blurring in the real optical setup. The other two reconstructed images somehow can be found residual blurring, especially Fig. 8(e) by the method C is the worst among them and dc term and twin-image can be found obviously.

Figures 8(b), 8(d) and 8(f) show the enlarged part of 8(a), 8(c) and 8(e), respectively.

The spatial frequencies and spatial resolutions of enlarged part are also shown in Table 2. Note that the spatial resolution of reconstructed image in Fig. 8(c) is about  $11.05\mu m$  which is the same level as published by Chen et al. [10]. Moreover, the contribution of the dc term and twin-image, which cause blurring as shown in Fig. 8(c) is less than before [10].

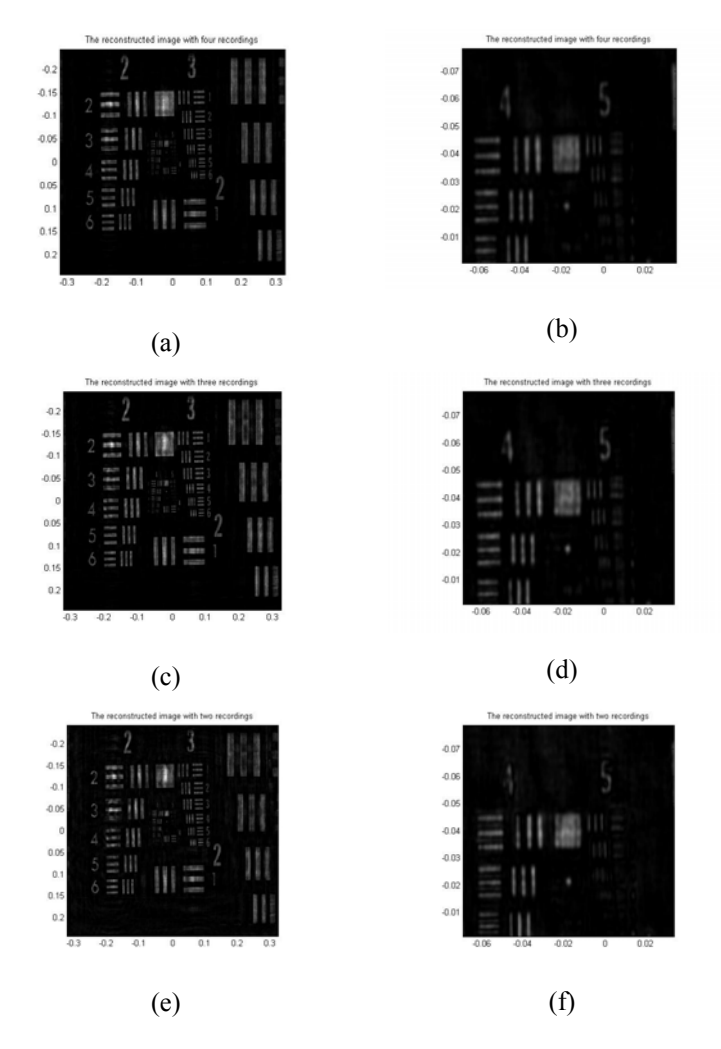


Fig. 8. Reconstructed images using: (a) and (b) Method A, (c) and (d) Method B, (e) and (f) Method C.

To validate the proposed approach, a simple experimental setup is performed. Instead of using the phase-shifting component, the phase-step  $\Delta \varphi$  of the reference wave is obtained by using a glass. The object wave, reference wave and two holograms with/without the phase-step are captured by CCD at the hologram plane, respectively. Secondly, following the proposed approach of our group [13], the  $\Delta \varphi$  value can be estimated easily from the pixels

array (515:525, 691:701) near the optical axis. The optimal estimated values of  $\Delta \varphi$  have to be selected by the try-by-error method and can not be generated automatically. Using Eqs. (8) and (9) with optimal values of  $\Delta \varphi$ , the spatial resolutions of the reconstructed images as shown in Figures. 8(b), 8(d) and 8(f), from our best understanding, apparently reach the state of art [10].

### V. CONCLUSIONS

We described the principle and algorithm for arbitrary phase-step digital holography using multiple holograms. Our proposed approach has been verified accurately with the simulation results. For the in-line geometry, we analyzed the parameters of the optical setup and used the simple argument to obtain the derivation of the arbitrary phase-step  $\Delta \varphi$ . With the estimated  $\Delta \varphi$ value, the object wavefront can be numerically reconstructed without blurring. We also evaluated the limitation of the pixel number which can be satisfied according to the given optical setup. Optical experiments were also performed to validate the approach. The optical results and spatial resolutions between different dc term suppression methods with recorded holograms are also presented and discussed. The proposed method will be further applied to phase objects, digital holographic microscopy, optical metrology, non-destructive testing etc.

#### **ACKNOWLEDGEMENTS**

The authors would like to thank the National Science Council of the Republic of China, Taiwan, for financially supporting this research under Contract No. **NSC** 96-2221-E-451-009-MY3. The authors would also like to thank Mr. Ji-Lu Huang for his help with the experimental setup and recording the holograms. They also appreciate the helpful comments and suggestions of the anonymous reviewers. Corresponding Author: Chi-Ching Chang's e-mail address is chichang@mdu.edu.tw.

### **REFERENCES**

- [1] Goodman J. W. and Lawrence R. W., "Digital image formation from electronically detected hologram," Appl. Phys. Lett. Vol. 11, pp. 77-79, 1967.
- [2] Schnars U. and Juptner W., "Direct recording of holograms by a CCD target and numerical reconstruction," Appl. Opt. Vol. **33**, pp. 179-181, 1994.
- [3] Kreis T. and Juptner W., "Suppression of the dc term in digital holography," Opt. Eng. Vol. **36**, pp. 2357-2360, 1997.
- [4] Chen G. L., Lin C. Y., Kuo M. K. and

- Chang C. C., "Numerical suppression of zero-order image in digital holography," Opt. Exp. Vol. **15**, pp. 8851-8856, 2007.
- [5] Takaki Y., Kawai H., and Ohzu H., "Hybrid holographic microscopy free of conjugate and zero-order images," Appl. Opt. Vol. 38, pp. 4990-4996, 1999.
- [6] Xu W., Jericho M. H., Meinertzhagen I. A., and Kreuzer H. J., "Digital in-line holography for biological applications," Proc. Natl. Acad. Sci. USA 98, pp. 11301-11305, 2001.
- [7] Xu W., Jericho M. H., Meinertzhagen I. A., and Kreuzer H. J., "Digital in-line holography of microspheres," Appl. Opt. Vol. **41**, pp. 5367-5375, 2002.
- [8] Garcia-Sucerquia J., Xu W., Jericho S. K., Klages P., Jericho M. H., and Kreuzer H. J., "Digital in-line holographic microscopy," Appl. Opt. Vol. 45, pp. 836-850, 2006.
- [9] Yamaguchi I. and Zhang T., "Phase-shifting digital holography," Opt. Lett. Vol. **22**, pp. 1268-1270, 1997.
- [10] Chen G. L., Lin C. Y., Yau H. F., Kuo M. K. and Chang C. C., "Wavefront reconstruction without twin-image blurring by two arbitrary step digital holograms," Opt. Exp. Vol. 15, pp. 11601-11607, 2007.
- [11] Meng X. F., Cai L. Z., Wang Y. R., Yang X. L., Xu X. F., Dong G. Y., Shen X. X. and Cheng X. C., "Wavefront reconstruction by two-step generalized phase-shifting interferometry," Opt. Commun. Vol. **281**, pp. 5701-5705, 2008.
- [12] Hsieh W. T., Kuo M. K., Yau H. F. and Chang C. C., "A simple arbitrary phase-step digital holography reconstruction approach without blurring using two holograms," Opt. Rev. Vol. 16, pp. 466-471, 2009.
- [13] Chang C. C., Hsieh W. T. and Kuo M. K., "Digital holography with arbitrary phase-step reconstruction using multiple holograms," Proc. SPIE, Vol. **7358**, pp. 735813-1-735813-11, 2009.
- [14] DeVelis J. B., Parrent, Jr. G. B., and Thompson B. J., "Image reconstruction with Fraunhofer holograms," JOSA Vol. **56**, pp. 423-427, 1966.
- [15] Schnars U. and Juptner W., "Digital

- recording and numerical reconstruction of holograms," Meas. Sci. Technol. Vol. **13**, pp. R85-R101, 2002.
- pp. R85-R101, 2002.
  [16] Fienup J. R., "Phase retrieval algorithms: a comparison," Appl. Opt. Vol. **21**, pp. 2758-2768, 1982.
- [17] Cuche E., Bevilacqua F., and Depeursinge C., "Digital holography for quantitative phase-contrast imaging," Opt. Lett. Vol. **24**, pp. 291-293, 1999.